Chemical Reviews

Volume 75, Number 5 October 1975

The Surface Composition of Binary Systems. Prediction of Surface Phase Diagrams of Solid Solutions

S. H. OVERBURY, P. A. BERTRAND, and G. A. SOMORJAI*

Inorganic Materials Research Division, Lawrence Berkeley Laboratory and Department of Chemistry, University of California, Berkeley, California 94720

Received May 15, 1974 (Revised Manuscript Received September 23, 1974)

Contents

I. Introduction

Of the various properties of surfaces, chemical composition is perhaps one of the most important that must be known in order to determine any other surface phenomena. Only recently, through the application of Auger electron spectroscopy, has it been possible to analyze the chemical composition of the top-most layer at the surface in vacuum or at the solid gas interface. This nondestructive technique can provide qualitative and quantitative surface chemical analysis with a sensitivity of about 1% of a monolayer (about 10^{-13} atom/cm^2), and it is now possible to compare the composition of the surface with the known bulk composition.

Simple thermodynamic arguments can convincingly demonstrate that the surface composition may be very different from the composition in the bulk for most multicomponent systems. Creation of a surface requires work, and it is always accompanied by a positive free energy change. Thus, in order to minimize the positive surface free energy, the surface will be enriched by the constituent which has the lowest surface free energy. This results, for many multicomponent systems, in gross imbalance between the surface composition in the top-most layer and in the bulk. Even for monatomic solids, this surface thermodynamic driving force is the cause of the segregation of impurities at the surface that lowers the total surface free energy.

In many important surface phenomena, such as heterogeneous catalysis or passivation of the surface by suitable protective coatings, the chemical composition of the top-most layer controls the surface properties and not the composition in the bulk. It is therefore necessary to develop thermodynamic models that permit prediction of surface composition of multicomponent systems as a function of bulk composition and as a function of temperature. Thus, we would like to determine the surface phase diagram.

In this paper we review the various thermodynamic models that permit practical determination of the surface composition of ideal or regular solid solutions. We shall summarize the experimental surface tension data available for metals, oxides, carbides, and organic solids, and we will point out the empirical correlations, if any, to other thermodynamic parameters that permit estimation of these important parameters when its direct experimental determination is difficult.

Finally, we shall review all of the experimental information available on the surface composition of alloys and using the models developed compute the surface phase diagrams for a few prototype systems.

II. Thermodynamic Models for Predicting Surface Compositions

With the aid of simplified models, it has been possible to predict the chemical composition in the first few layers at the surface of a homogeneous binary solid solution. These theories may be applied to predict the surface composition of alloys or the segregation of impurities on an otherwise nearly pure crystal. Perhaps the most widely known is the monolayer model[1] in which the top-most surface layer is treated as distinct from all the other layers. All the inner layers are assumed to have the bulk composition. An expression is then written for the chemical potentials of the surface and bulk phases, and these chemical potentials are then equated to give an expression for the surface composition. Utilizing this model, the surface layer and the bulk may be treated as ideal or as regular solutions.

In the multilayer model, the two-component crystal is treated as an infinite set of layers of atoms (or molecules), and each layer is treated as having a possibly different composition ratio. An expression is then written for the free energy of the system with the atom fractions of each layer inserted as variable parameters which are varied to obtain the minimum free energy for the whole system. For ease of computation, the process may be truncated below a set number of layers, with all deeper lying layers then assumed to have the bulk composition. Again, each of the layers may be treated as part of an ideal or regular solution. These models have been applied to liquid alloy solutions,[2] and to solid–liquid and vapor–liquid interfaces,[3-5] but may also be expected to yield the surface composition of solid binary solutions at a solid–vapor or solid–vacuum interface.[6]

As an example, we shall outline here a derivation of the surface composition of an ideal solution in the monolayer model approximation. The solution is treated as having two phases, a surface monolayer phase s, and a bulk phase b. The bulk phase has a known atom fraction x_1^b of component one, and $x_2^b = (1 - x_1^b)$ for component two. We define the free energy functions for the bulk and surface phases as follows:

$$G^s = E^s - TS^s + PV^s = \sum_{i=1}^{2} \mu_i^s n_i^s + \sigma A$$

$$G^s = E^s - TS^s + PV^s - \sigma A = \sum_{i=1}^{2} \mu_i^s n_i^s$$

$$G^b = G^b = E^b - TS^b + PV^b = \sum_{i=1}^{2} \mu_i^b n_i^b$$

Here all symbols have their usual meaning; σ is the surface tension and A is the surface area. Then the chemical potential of the surface phase is

$$\mu_i^s = \left.\frac{\partial G}{\partial n_i^s}\right|_{T,P,n_j^s \neq n_i^s,\sigma} = \left.\frac{\partial (G^b + G^s)}{\partial n_i^s}\right|_{T,P,n_j^s \neq n_i^s,\sigma} = \left.\frac{\partial G^s}{\partial n_i^s}\right|_{T,P,n_j^s \neq n_i^s,\sigma} = \left.\frac{\partial (G^s - \sigma A)}{\partial n_i^s}\right|_{T,P,n_j^s \neq n_i^s,\sigma} = \left.\frac{\partial G^s}{\partial n_i^s}\right|_{T,P,n_j^s \neq n_i^s,\sigma} - \sigma a_i$$

where

$$a_i = \left.\frac{\partial A}{\partial n_i^s}\right|_{T,P,n_j^s \neq n_i^s,\sigma}$$

Similarly for the bulk

$$\mu_i^b = \left.\frac{\partial (G^b + G^s)}{\partial n_i^b}\right|_{T,P,n_j^b \neq n_i^b} = \left.\frac{\partial G^b}{\partial n_i^b}\right|_{T,P,n_j^b \neq n_i^b} = \left.\frac{\partial G^b}{\partial n_i^b}\right|_{T,P,n_j^b \neq n_i^b}$$

but $G^b = \sum \mu_i^b n_i^b$ so that for an ideal solution

$$G^b = G^b = \sum_{i=1}^{2} n_i^b \mu_i^b = \sum_{i=1}^{2} n_i^b (\mu_i^{0,b} + RT \ln x_i^b)$$

where the property of ideal solution that $\mu_i^b = \mu_i^{0,b} + RT \ln x_i^b$ has been used, where $\mu_i^{0,b}$ is the chemical potential of pure i in its standard state. Let us assume that by analogy

$$G^s = \sum_{i=1}^{2} n_i^s (\mu_i^{0,s} + RT \ln x_i^s)$$

where x_i^s is the atom fraction of i in the surface phase. Then

$$\mu_i^s = \left.\frac{\partial G^s}{\partial n_i^s}\right|_{T,P,n_j^s \neq n_i^s,\sigma} - \sigma a_i = \mu_i^{0,s} + RT \ln x_i^s - \sigma a_i$$

The condition for equilibrium is that $\mu_i^s = \mu_i^b$, so that

$$\mu_i^b = \mu_i^{0,b} + RT \ln x_i^b = \mu_i^{0,s} + RT \ln x_i^s - \sigma a_i$$

For the case in which $x_i^s = x_i^b = 1$ we have

$$\mu_i^{0,s} - \mu_i^{0,b} = \sigma_i a_i$$

where σ_i is the surface tension of pure i. Using this in the preceding equation, and if we assume that $a_1 = a_2 = a$, then for a two-component system, we have the equations

$$\sigma a = \sigma_1 a + RT \ln x_1^s - RT \ln x_1^b$$

$$= \sigma_2 a + RT \ln x_2^s - RT \ln x_2^b$$

This can be rewritten as

$$\frac{x_2^s}{x_1^s} = \frac{x_2^b}{x_1^b} \exp\left(\frac{(\sigma_1 - \sigma_2)a}{RT}\right) \quad (1)$$

and this is the final result for the monolayer ideal solution model.

Equation 1 is modified by treating the two-component system as a regular solution.[7,8] The regular solution monolayer model is derived by calculating the total bonding energy of a given composition with a surface atom fraction x_1^s and x_2^s and the bulk atom fraction. The bond energies between the atoms are E_{11}, E_{22}, and E_{12} where E_{11} is the bond energy per mole for bonds between atoms of type one, etc. The expression for the bonding energy is used to find an expression for the chemical potential for the surface layer, which is equated to the chemical potential for the bulk. The resulting equation is[1]

$$\frac{x_2^s}{x_1^s} = \frac{x_2^b}{x_1^b} \exp\left\{\frac{(\sigma_1 - \sigma_2)a}{RT}\right\} \exp\left\{\frac{\Omega(l+m)}{RT} \times \left[(x_1^b)^2 - (x_2^b)^2\right] + \frac{\Omega l}{RT}\left[(x_2^s)^2 - (x_1^s)^2\right]\right\} \quad (2)$$

where l is the fraction of nearest neighbors to an atom in the plane, and m is the fraction of nearest neighbors below the layer containing the atom. For example, for an atom with $z = 12$ nearest neighbors (three above, three below, and six in the same plane), then $l = 6/12 = 0.5$ and $m = 3/12 = 0.25$. (This is the configuration for the (111) face of an fcc solid.) Ω is the regular solution parameter and is given by

$$\Omega = z\left(E_{12} - \frac{E_{11} + E_{22}}{2}\right)$$

The multilayer model described earlier has a rather complicated form and will not be given here. The interested reader is referred to the references mentioned earlier.[3-6]

In all of the models presented above, it is assumed that the binary solid is homogeneous. If there are large differences in interaction energies E_{12} and the energies E_{11} and E_{22}, that is, if the regular solution parameter is very large, then it may be expected that there will be either phase separation or there will be ordering. In either of these two cases, these models are not directly applicable. In the case of phase separation, if the resulting phases are homogeneous, each phase may still independently obey one of the above models. These considerations indicate that in order to determine a surface phase diagram of a solid solution, the bulk phase diagram should already be known.

III. Surface Tensions of Solids and Liquids: Review of Experimental Data and Methods of Estimation

One of the major difficulties in applying the above models to compute the surface composition of multicomponent sys-

TABLE I. Values of the Parameters for Eq 3 and 4 That Give the Best Least-Squares Fit to the Experimental Surface Tension Data for Several Liquid Metals

	Corresponding states			Linear			
Metal	σ_0, ergs/cm^2	T_c, °K	$1 + R$	σ_0, ergs/cm^2	$\partial\sigma/\partial T$	T_c, °K	Ref
Al	943.85	14,481	1.22	943.17	0.0782	12,061	*a, b*
Sb	403.17	12,834	1.22	402.78	0.0375	10,741	*a, b*
Bi	416.44	7,719	1.25	415.54	0.0656	6,334	*a, b*
Cd	700.54	6,736	1.22	699.35	0.1238	5,649	*a, b*
Cs	86.78	1,958	1.19	85.57	0.0491	2,087	*a, c, d*
Cu	1291.81	63,540	1.21	1291.46	0.0244	52,927	*a, b*
Pb	489.06	9,106	1.27	488.15	0.0663	7,363	*a, b*
Li	483.27	3,316	1.23	475.88	0.1640	2,902	*c*
Mg	656.34	6,350	1.22	654.09	0.1217	5,375	*a, b*
K	144.06	3,126	1.03	138.52	0.0739	1,898	*c, d*
Rb	105.52	2,185	1.33	103.56	0.0573	1,807	*c, d*
Ag	1277.11	5,333	1.22	1262.43	0.2729	4,626	*a, b, e*
Na	252.51	2,452	1.22	249.73	0.1161	2,151	*a–c*
Sn	578.30	11,876	1.22	577.93	0.0585	9,879	*a, b, e*
Zn	832.74	9,703	1.25	830.89	0.1037	8,012	*a, b*

[a] "Handbook of Chemistry and Physics," 53rd ed, Chemical Rubber Publishing Co., Cleveland, Ohio, 1972. [b] V. K. Sementchenko, "Surface Phenomena in Metals and Alloys," Pergamon Press, New York, N.Y., 1962. [c] J. Bohdansky and H. E. J. Schins, *J. Inorg. Nucl. Chem.*, **29**, 2173 (1967). [d] Yu. P. Osminin, *Zh. Fiz. Khim.*, **44**, 1177 (1970). [e] "International Critical Tables," McGraw-Hill, New York, N.Y., 1928.

tems is the lack of availability of reliable surface tension data for solids. The surface tension σ is the reversible work required to create a unit area of surface at constant temperature, volume, and chemical potential. The surface area may be increased by adding more atoms (or molecules) to the surface, or by stretching the existing surface. Depending on the experimental conditions during a surface tension experiment, one may measure a combination of surface stress and surface tension of the solid surface. The difficulty in distinguishing between surface stress and surface tension experimentally is removed for liquids because the diffusion of atoms in the liquid is fast enough to remove the stress. Also, since adsorbed impurities will alter the surface tension, markedly, surface cleanliness is a very important factor in these experiments.

Another problem in utilizing the experimentally determined surface tension data for solids is the lack of data as a function of temperature. Most available values are for rather high temperatures, for $T/T_m > 0.7$, where T_m is the melting point of the solid.[9] The temperature dependence of the surface tension may be significant over large temperature ranges and it is usually unknown. Empirical expressions for the temperature dependence of surface tension have been formulated in Eötvös' Law[10] and its modified versions by Ramsey and Shields[11] and of Katayama,[12] and these rules have been applied to solids.[13] Guggenheim has also derived an equation that gives the functional behavior of σ with T.[14]

The surface tension of the solid surfaces will, in general, depend on the crystallographic orientation. This coupled with the effect of crystallite size (that is, the influence of curvature on surface tension) further increases the difficulty of obtaining reliable surface tension data.

We have listed the surface free energies that are reported for over 20 liquid and solid metals and have found a useful correlation that permits estimation of the surface tension of metals to within 8% from the well-known heats of vaporization and sublimation. This correlation, as observed and reviewed by others,[15] can then be used to estimate unknown surface free energies and to predict the surface compositions of several solid solutions that are commonly utilized or to calculate other thermodynamic parameters of the studied systems.

A. Surface Tension of Liquid Metals

The surface tension of many liquid metals has been measured over the past decade.[16,17] The surface tension was frequently determined as a function of temperature in a finite temperature range. The surface tension of liquid metals decreases with increasing temperature, and of course it must vanish at the critical point, T_c. One equation used to describe this behavior is the Guggenheim equation[14] which is based on the corresponding states principle:

$$\sigma = \sigma_0[1 - (T/T_c)]^{1+R} \quad (3)$$

where σ_0, R, and T_c are parameters adjusted to give the best fit to the experimental data. R is usually taken as equal to 2/9. Another equation frequently employed, especially to determine interfacial tension, assumes linear temperature dependence:

$$\sigma = \sigma_0 - (\partial\sigma/\partial T)_P T \quad (4)$$

This equation derives from the expression of the Gibbs specific surface free energy, $G^s(T) = H^s - TS^s$, since for the one-component system $\sigma(T) = G^s(T)$, $S^s = -(\partial\sigma/\partial T)_P$, and $\sigma_0 = H_0{}^s$. For the case when H^s and S^s are independent of temperature, it is possible to obtain both functions from the temperature dependence of σ. The intercept of the straight line (σ vs. T) at absolute zero, σ_0, yields a specific surface enthalpy, and the slope, $(d\sigma/dT)_P$, is the specific surface entropy.

The first three columns of Table I show the values of the parameters of the Guggenheim equation (σ_0, T_c, $1 + R$) that give the best least-squares fit to the experimental surface tension values for 15 different metals. The last three columns of Table I give the values of the parameters σ_0 and $(\partial\sigma/\partial T)_P$ in eq 4 that give the best fit to the same data. The references identify sources of experimental data. The σ_0 values that were determined from fitting the experimental values to both equations are almost identical. Thus, one has no reason to prefer one equation over the other on this basis. The two equations give different results in their prediction of the critical temperature. This is due to the different functional dependence of σ on T and the long extrapolation required to reach the point where the surface tension is zero. The linear and Guggenheim relations are equally accurate in the region where data are available, but they begin to deviate at about 1000–3000°K, depending on the metal.

Although the temperature dependence of the surface tensions of liquid metals are certainly not negligible, inspection of the $(\partial\sigma/\partial T)_P$ values listed in Table I reveals that most surface

TABLE II. Densities, Molar Surface Areas, Heats of Vaporization, and Calculated and Experimental Values of σ_l for Several Liquid Metals

Metal	ρ, g/cm^3[a]	A, cm^2/mol	ΔH_{vap}, ergs/mol[a]	σ_l(calcd), ergs/cm^2	σ_l(exptl), ergs/cm^2	
					This paper	Others
Al	2.39	4.61×10^8	2.90×10^{12}	937	870	914,[b] 825,[a] 860,[a] 865[a]
Sb	6.48	6.67×10^8	2.00×10^{12}	447	369	383[a]
Bi	10.05	7.13×10^8	1.75×10^{12}	366	380	378,[a] 376[c]
Cs	1.85	16.8×10^8	0.69×10^{12}	61	58	60[a]
Cu	7.95	3.68×10^8	3.11×10^{12}	1259	1258	1270,[a] 1300,[a] 1220,[d] 1350[d]
Ir	20.0	4.16×10^8	5.86×10^{12}	2113		2250[d]
Pb	10.70	6.63×10^8	1.82×10^{12}	409	448	451[a]
Li	0.52	5.3×10^8	1.39×10^{12}	391	400	
Mo	9.33	4.44×10^8	6.16×10^{12}	2081		2250,[d] 2080[d]
Ni	7.8	3.54×10^8	3.79×10^{12}	1606		1780,[d] 1725,[d] 1720[d]
Nb	7.83	4.95×10^8	6.99×10^{12}	2118		1900[d]
Pd	10.7	4.26×10^8	3.74×10^{12}	1317		1500[d]
Pt	19.7	4.25×10^8	5.12×10^{12}	1807		1800,[d] 1699,[d] 1865,[d] 1740[d]
K	0.82	12.4×10^8	0.81×10^{12}	97	114	114[e]
Rh	11	4.08×10^8	5.33×10^{12}	1960		2000[d]
Rb	1.45	14.1×10^8	0.78×10^{12}	82	86	76,[a] 92[e]
Ag	9.33	4.74×10^8	2.59×10^{12}	814	926	785,[a] 930[f]
Na	0.93	7.77×10^8	1.00×10^{12}	192	207	206,[c] 220,[f] 191[a]
Ta	15.0	4.97×10^8	7.34×10^{12}	2215		2150,[d] 2360,[d] 2020[d]
Sn	7.00	6.24×10^8	2.35×10^{12}	561	549	526,[a] 550[b]
W	17.6	4.53×10^8	7.84×10^{12}	2596		2500[d]
V	5.55	4.15×10^8	4.82×10^{12}	1742		1950[d]

[a] "Handbook of Chemistry and Physics," 53rd ed, Chemical Rubber Publishing Co., Cleveland, Ohio, 1972. [b] V. K. Sementchenko, "Surface Phenomena in Metals and Alloys," Pergamon Press, New York, N.Y., 1962. [c] A. Bondi, *Chem. Rev.*, **52**, 417 (1953). [d] B. C. Allen, *Trans. Met. Soc. AIME*, **227**, 1175 (1963). [e] Yu. P. Osminin, *Zh. Fiz. Khim.*, **44**, 1177 (1970). [f] A. W. Adamson, "The Physical Chemistry of Surface," Interscience, New York, N.Y., 1960.

tensions change by no more than 5% in a 100° temperature interval. This variation is not greater than the uncertainty of most surface tension experiments. Thus, the surface tension may be taken as constant in most cases, as long as the temperature range of experimental interest is limited.

There are anomalies reported in measurements of the temperature dependence of σ that indicate deviations from the straight line σ *vs.* T behavior. A change of slope of the σ *vs.* T curve indicates a change of surface entropy that may signify ordering on the surface. The consideration of these anomalies is outside the scope of this paper.

B. Correlation between Surface Tension of Liquid Metals and Their Heats of Vaporization

The specific surface free energy for an unstrained phase is equal to the increase of the total free energy of the system per unit increase of the surface area: $G^s = (\partial G/\partial A)_{T,P}$. Thus, creation of more surface always increases the total free energy of the system. Since atomic bonds must be broken to create surfaces, it is expected that the specific surface free energy be related to the heat of vaporization, which reflects the energy input necessary to break all the bonds of atoms in the condensed phase. The heat of vaporization is a molar quantity (energy/g-atom), while the specific surface free energy is defined as energy per unit area (energy/cm^2). In order to compare the two values, we must convert the specific surface free energy to molar surface free energy (energy/g-atom).[18] Because of differences in the densities of various materials, they will have differing numbers of atoms occupying a unit area. Let us define an area, A, as the area occupied by Avogadro's number of atoms, N. The atomic volume V_a is given by

$$V_a = V_m/N = M/N\rho \tag{5}$$

where V_m is the molar volume, ρ the density, and M the atomic weight. Thus the area per atom A_a is given by[18]

$$A_a = f(V_a)^{2/3} = f(M/N\rho)^{2/3} \tag{6}$$

where f is a structure factor that corrects for the assumption that the surface is the (100) face of a simple cubic lattice as was implicitly assumed in using $V^{2/3}$ as the surface area. [Following McLachan,[19] the area of an atom is expected to be proportional to the square of some dimension of the atom and the volume proportional to its cube: $A = bD^2$, $V = cD^3$. Thus $A = (b/c^{2/3})V^{2/3}$. For the (100) face of a simple cubic structure $b = c = 1$, so $f = 1$ as expected. For the (111) face of an fcc metal, $b = \sqrt{3}/4$ and $c = 1/4$, which yields $f = 1.09$.] The value of f is 1.09 for melts of fcc solids, 1.12 for melts of bcc solids, and 1.14 for molten Bi, Sn, and Sb (orthorhombic in the solid state).[18] The molar surface area is then given by

$$A = NA_a = fN^{1/3}(M/\rho)^{2/3} \tag{7}$$

and the molar surface tension or molar surface free energy of the liquid is defined as

$$\sigma_{lm}(T) = A\sigma_l(T) \tag{8}$$

Now we can proceed to compare σ_{lm} directly to the heat of vaporization since both quantities are known from experiments for the 22 liquid metals that are listed in Table II. The plot σ_{lm} at the melting point for each metal vs. their heats of vaporization is shown in Figure 1. A least-squares fit yields the relationship

$$\sigma_{lm} = 0.15\Delta H_{vap} \tag{9}$$

All of the experimental data fit this equation with a standard deviation of 8%.

C. Correlation between the Surface Tension of Solids and Their Heats of Sublimation

For monatomic solids surface tension determination is more difficult, and the available experimental data are scarce

TABLE III. Densities, Molar Surface Areas, Heats of Sublimation, and Calculated and Experimental Values of σ_s for Several Metallic Solids

Metal	ρ, g/cm^3[a]	A, cm^2/mol	ΔH_{sub}, ergs/mol[b]	σ_s, ergs/cm^2 Calcd	σ_s, ergs/cm^2 Exptl	T (°K) of σ_s (exptl)
Al	2.70	4.24 x 10^8	3.14 x 10^{12}	1198	1140 ± 200[c]	450
Cu	8.96	3.7 x 10^8	3.39 x 10^{12}	1484	1670[d]	1320
					1710[e]	1273
					1750[f]	1173
Au	19.3	4.44 x 10^8	3.68 x 10^{12}	1343	1400 ± 65[g]	1315, 1290
					1370 ± 150[h]	1313
					1410[d]	1300
Ni	8.90	3.22 x 10^8	3.39 x 10^{12}	1706	1850[d]	1523
					1860 ± 200[i]	1493
Nb	8.60	4.56 x 10^8	7.20 x 10^{12}	2557	2100 ± 100[d,j]	2523
					2550 ± 550[k]	1773
Pt	21.45	4.06 x 10^8	5.56 x 10^{12}	2219	2300 ± 800[l]	1310
					2340[d]	1311
Ag	10.5	4.34 x 10^8	2.85 x 10^{11}	1064	1140 ± 90[d,m]	1203, 1180
Ta	16.6	4.64 x 10^8	7.78 x 10^{12}	2713	2680 ± 500[k]	1773
Sn	5.76	6.89 x 10^8	2.30 x 10^{11}	541	600 ± 75[n]	488
Ti	4.5	4.47 x 10^8	4.73 x 10^{12}	1712	1700[o]	1873

[a] "International Critical Tables," McGraw-Hill, New York, N.Y., 1928. [b] A. N. Nesmeyanov, "Vapor Pressure of the Chemical Elements," Elsevier Publishing Co., New York, N.Y., 1963. Also, much sublimation data are compiled in Hultgren's work (ref 82). [c] R. E. Smallman, K. H. Westmacott, and P. S. Dobson, *Metal Sci. J.*, 2, 177 (1968). [d] J. M. Blakeley and P. S. Maiya in "Surfaces and Interfaces," J. J. Burke et al., Ed., Syracuse University Press, Syracuse, N.Y., 1967. [e] H. Udin, A. J. Schaler, and J. Wulff, *Trans. AIME*, 185, 186 (1949). [f] J. H. Hoage, U. S. Atomic Energy Commission Report, No. HW-78132, (1963). [g] F. H. Buttner, H. Udin, and J. Wulff, *Trans. AIME*, 191, 1209 (1951). [h] E. D. Hondros and R. Gladman, *Surface Sci.*, 9, 471 (1968). [i] J. M. Blakely and P. S. Maiya, *J. Appl. Phys.*, 38, 698 (1967). [j] S. V. Radcliff, *J. Less-Common Metals*, 3, 360 (1961). [k] E. M. Hodkin, M. C. Nicholas, and D. M. Poole, *J. Less-Common Metals*, 20, 93 (1970). [l] J. M. Blakely and H. Mykura, *Acta Met.*, 10, 565 (1962). [m] E. R. Funk, H. Udin, and J. Wulff, *Trans. AIME*, 191, 1206 (1951). [n] E. D. Greenhill and S. R. McDonald, *Nature (London)*, 171, 37 (1953). [o] V. I. Kostikov, A. V. Kharitonov, and V. Z. Savenko, *Phys. Met. Metallogr.*, 26, 181 (1968).

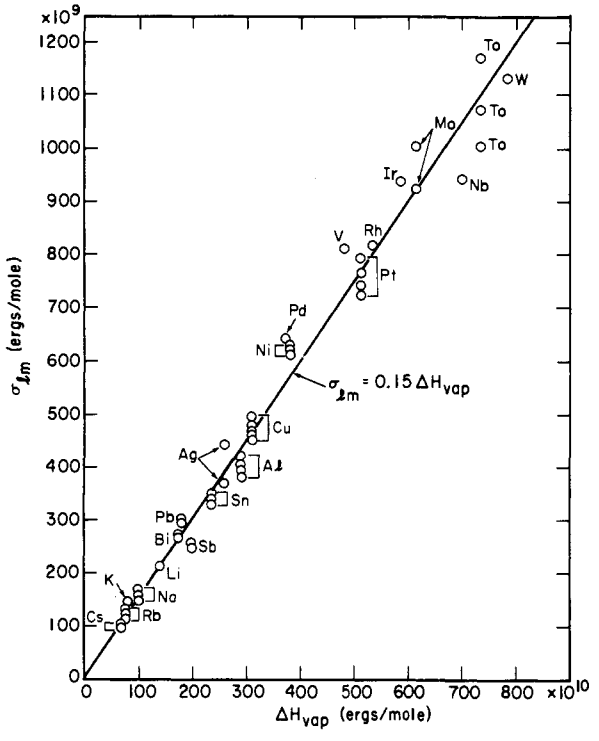

Figure 1. Molar surface energy of liquid metals, σ_{lm}, as a function of their heats of vaporization.

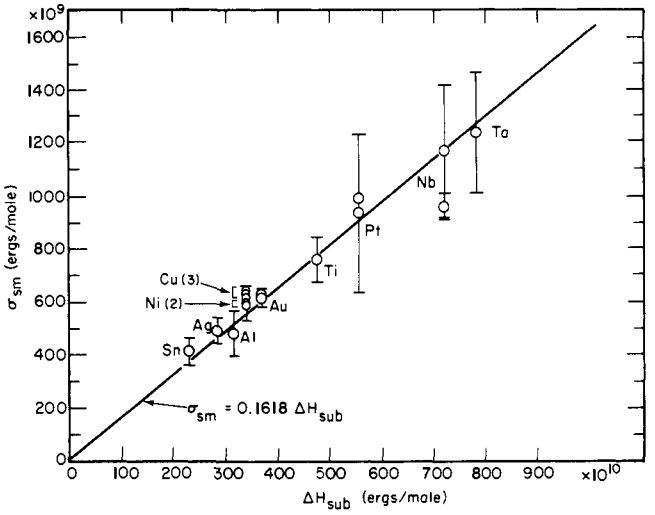

Figure 2. Molar surface energy of several solid metals as a function of their heats of sublimation.

and often determined only at one temperature.[20] Nevertheless, we have collected most of the available data, which are tabulated in Table III. In Figure 2 the molar surface tensions of the solids, σ_{sm}, are plotted against the heats of sublimation, ΔH_{sub}, for various metals. A least-squares fit yields the relationship

$$\sigma_{sm} = 0.16 \Delta H_{sub} \quad (10)$$

The temperature dependence of σ_{sm} was disregarded in the correlation as discussed earlier. The validity of this approximation can be seen by examining the data for copper and nickel; the correction for the temperature dependence is well within the experimental error. There is excellent agreement between the experimental values and those calculable from eq 10, and the standard deviation is 8%. Thus it appears that at least for monatomic solids the surface tension may be estimated when direct experimental determination is difficult or lacking.

D. Surface Tension Data for Organic Liquids, Oxides, and Carbides

The correlation (σ vs. ΔH) that holds so well for metals does not hold for organic liquids of various types. This must

TABLE IV. Values of Parameters for Eq 3 and 4 That Give the Best Least-Squares Fit to the Experimental Surface Tension Data for Several Organic Liquids

	Corresponding states			Linear		
Compound[a,b]	σ_0, ergs/cm²	T_c, °K	$1 + R$	σ_0, ergs/cm²	$\partial\sigma/\partial T$	T_c, °K
C_2H_2	73.38	287	1.22	64.64	0.2380	272
CH_3OCH_3	61.81	397	1.22	56.64	0.1530	370
CH_2CH_2O	76.86	480	1.22	72.54	0.1646	441
$(CH_3)_2NH$	44.52	522	1.22	42.87	0.0910	471
$(CH_3)_3N$	48.37	472	1.22	46.13	0.1074	430
$C_2H_5NH_2$	51.86	563	1.34	49.02	0.1019	481
CO	29.57	131	1.75	27.22	0.2266	120
$CHCl_3$	72.00	523	1.18	67.47	0.1373	491
HCN	59.97	466	1.22	54.95	0.1266	434
HCOOH	71.91	711	1.22	69.17	0.1077	642
CH_3COOH	58.17	593	1.08	55.90	0.0962	581
C_2H_5COOH	57.24	631	1.22	53.75	0.0925	581
CH_3CHO	64.67	467	1.13	61.22	0.1366	448
CH_3COCH_3	63.99	507	1.15	60.46	0.1254	482
$C_2H_6O_2$	77.35	889	1.21	75.55	0.0952	794
$HCOOC_2H_5$	66.03	508	1.20	57.67	0.1168	494
CH_3COOCH_3	70.71	507	1.22	60.48	0.1230	492
n-C_6H_{14}	51.97	494	1.15	49.02	0.1041	470
n-C_8H_{18}	53.75	561	1.22	50.69	0.0985	515
C_5H_5N	86.40	598	1.22	81.17	0.1476	550
$C_6H_5NO_2$	82.60	775	1.33	77.23	0.1140	678
C_6H_5OH	79.70	704	1.11	72.75	0.1086	670
$C_6H_5NH_2$	80.38	729	1.22	76.68	0.1153	665
C_6H_5CHO	76.80	709	1.22	74.22	0.1167	636
$C_6H_5CH_3$	62.21	606	1.21	58.65	0.1048	560

[a] "Handbook of Chemistry and Physics," 53rd ed, Chemical Rubber Publishing Co., Cleveland, Ohio, 1972. [b] "International Critical Tables," McGraw-Hill, New York, N.Y., 1928.

be due to the diverse bonding characteristics and packing of these liquids. The first three columns of Table IV give the values of the parameters σ, T_c, and $1 + R$ of the Guggenheim equation that give the best least-squares fit to the experimental surface tension values for 25 organic liquids. The last three columns of Table IV show the values of the parameters of eq 4 [σ_0 and $(\partial\sigma/\partial T)_P$] that give the best fit to the same data.

In Table V we list the surface free energies of several oxides and some carbides. For these solids there was no good correlation between the surface tension and the heat of vaporization. Finally, the interested reader is referred to extensive collected surface tension data for molten salts.[21]

E. Physical Basis for Surface Tension Correlations

The surface free energy is defined as the increase of the total free energy of the system per unit increase of the surface area. For metals, the creation of more surface requires the breaking of chemical bonds which is accompanied by charge redistribution of the electron gas. Theoretical computations of the surface tension of metals have been performed by considering these contributions separately.

The model which takes into account only the breaking of chemical bonds correlates the surface tension with the heat of vaporization or heat of sublimation. Skapski[18] and McLachan[19] considered the breaking of only the nearest neighbor bonds in the condensed phase. For a close-packed plane of a solid[72] an atom in the surface has nine bonds to the interior of the solid; thus, the heat of sublimation corresponds to the energy necessary to break 18 half-bonds. The surface free energy is approximately equal to the energy of breaking the bonds by transferring a bulk atom to the surface; since this is a close-packed solid (12 nearest neighbors in total), there will be 3 half-bonds per atom directed out of the plane at the interface. Thus the ratio of σ_{sm} to ΔH_{sub} should be 3:18 or 1/6, which is approximately the same as the empirically determined value that is given in eq 10. Such a simple model does not explain the surface tension of organic substances as these simple assumptions are no longer valid. More detailed calculations should take into account longer range interactions, relaxation of the newly created surface atoms into their new equilibrium positions, and the excess of binding energy the surface atoms may have as compared to those in the bulk due to the availability of surplus bonding orbitals.[73] Such a model, when developed, would include both the bond breaking and the charge redistribution that take place on creating new surfaces.

The simplest version of the free electron gas model used to calculate the charge redistribution that takes place at the freshly made surface is the particle in a box, with the surfaces of the metal corresponding to the walls of the box, which contains a uniform density of electrons.[74] This model was improved by various workers,[75,76] but until Hohenberg, Kohn, and Sham[77,78] devised a more general formalism which can treat inhomogeneous electron distributions, the change of electron density at the surface of a metal was ignored. Using this new model Lang and Kohn[79] predicted metal surface free energies within about 25% of the experimental values. More recently Schmit and Lucas[80,81] proposed that the surface free energies of metals are mainly due to the change in plasmon density caused by the introduction of a new surface. Their computed surface free energies fall within 30% of the measured values, and there is no attempt to fit the experimental data.

These different types of calculations of the surface tensions of metals provide the physical basis of the observed correlation between surface tension and the heat of vaporization or heat of sublimation. It appears that eq 9 and 10 can be used with confidence to estimate surface tensions and utilize them in evaluating many important properties of surfaces, their composition, adhesion, or other surface thermodynamic parameters.

IV. Predicted Surface Compositions

In section II we have shown some of the models that have been developed to predict surface compositions. The most important parameter in these models was the difference in surface tensions of the two components. Having obtained this quantity, by independent measurements, and the molar surface area, which can be calculated from well-known density data (see eq 7), it is easy to calculate the surface composition predicted by the monolayer ideal solution model. (As stated earlier, in the derivation of the monolayer models, it is assumed that the surface areas of both pure components are equal. Calculating these surface areas from density data also assumes that there is no surface reconstruction.) In addition, if the solution under study is believed to behave more like a regular solution (if the heat of mixing is not zero), then only the regular solution parameter and knowledge of crystal packing are necessary to calculate the surface composition predicted by the monolayer regular solution model. The packing information is obtained from the crystal structure and the crystallographic face which is being studied. The regular solution parameter, Ω, can be obtained from heats of mixing since[7]

$$\Omega = \Delta H_{mixing}/x_1x_2$$

For binary metallic alloy systems these heats of mixing are tabulated.[82]

In the following, we will present calculations of surface

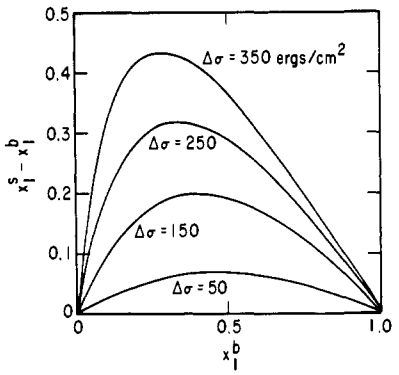

Figure 3. Surface enrichment for various valves of $\Delta\sigma = \sigma_2 - \sigma_1$ at $T = 1000°K$, in the ideal solution monolayer model approximation.

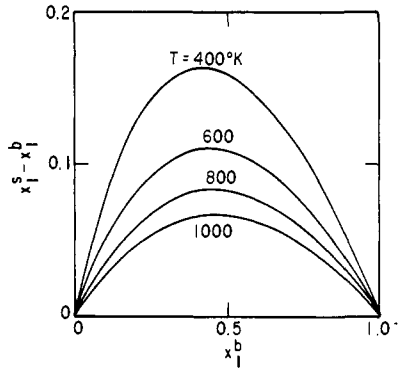

Figure 4. Surface enrichment at selected temperatures of a system with $\sigma_2 - \sigma_1 = 50$ ergs/cm^2 in the ideal solution monolayer model approximation.

composition of model systems. The parameters involved will be varied in order to yield a more thorough understanding and a qualitative feeling for the model predictions. Following this, in section V, results for systems which have been studied using Auger electron spectroscopy will be presented and these results compared with the predicted values for the surface compositions.

The most important parameter in the models is the surface tension or surface free energy difference. In Figure 3, the enrichment of the surface monolayer, that is, the quantity $x_1^s - x_1^b$, where x stands for atom fraction, is calculated as a function of the bulk composition of the system. Here the subscript 1 is assigned to the component with the lowest surface energy. The enrichment was calculated using the monolayer model and assuming that the solution is ideal ($\Omega = 0$). The area and the temperature were fixed at 4.4 × 10^8 cm^2/mol and 1000°K, respectively. It can be seen that for a surface energy difference of 150 ergs/cm^2, the surface excess is 20% for the component with the lowest surface free energy (for a solution with an overall bulk composition of 40% of the low surface energy component). In metal alloys, surface energy differences as great as 150 ergs/cm^2, and even larger, are in fact quite common. It is this large effect that creates a situation in which the surface composition may be very different from the bulk composition. In addition, the effect is important throughout a large bulk composition range.

In these calculations the temperature was fixed at 1000°K. It is interesting, however, to see how the results vary with temperature. In Figure 4, the surface energy difference was fixed at a value of 50 ergs/cm^2. This calculation is again for the monolayer model and assumes that the solutions are ideal. The surface area remained fixed at 4.4 × 10^{8}cm^2/mol. It is immediately apparent that the surface enrichment is of greatest magnitude at low temperatures and that the enrichment is strongly temperature dependent. Halving the temperature causes the surface enrichment to approximately double. Thus the surface effect is of greatest importance at temperatures where typical catalytic reactions are run. One experimental check of the monolayer model would be to measure the temperature dependence of the surface composition of an alloy. From the form of eq 1 it can easily be seen that if the surface energy is either independent of temperature or varies linearly with temperature, then a plot of ln (x_2^s/x_1^s) vs. $1/T$ should be linear (assuming area is not a function of T). Experimentally determined temperature dependence of this type then is experimental evidence supporting the monolayer–ideal solution model.

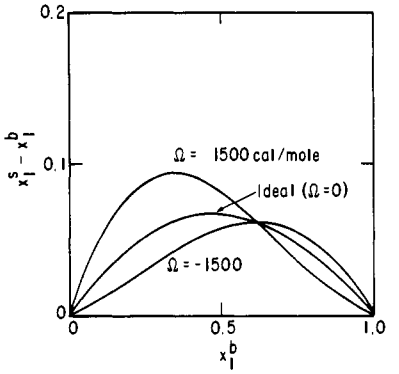

Figure 5. Surface enrichment for an fcc (111) surface of a system with $\sigma_2 - \sigma_1 = 50$ ergs/cm^2 at 1000°K and different values of the regular solution parameter in the monolayer model approximation.

All the calculations that were discussed above were for ideal solutions. For regular solutions, the expression describing the concentrations of the surface monolayer is more complicated, and the results are less obvious from the equation (eq 2). To clarify, the composition of the surface layer is calculated for positive (endothermic) and negative (exothermic) values of the regular solution parameter and is compared with the ideal solution result. This is shown in Figure 5. In this calculation, the system was assumed to be face-centered close-packed, and the surface energy difference was fixed at 50 ergs/cm^2. The area and the temperature were again fixed at 4.4 × 10^{8}cm^2/mol and 1000°K, respectively. The regular solution parameter affects the magnitude of the enrichment, especially for positive values of Ω. The value of 1500 cal/mol for Ω is actually a bit large for that expected for a homogeneous solid solution. For most alloys, phase separation may be expected if the magnitude of Ω is much larger. For this value, however, it is seen that there is an appreciable departure from the predictions of the ideal solution model.

It is likely that if such strong surface enrichment takes place in the surface monolayer, some alteration of the adjacent inner layers will also occur. An improved model is the multilayer model, and to demonstrate results of multilayer calculations we reproduce here some calculations made by Williams.[6] In this work, values for heats of sublimation are used directly in the calculations, instead of experimental surface tension data. We have already shown the validity of this approach. The factors which relate the surface energy to the heats of sublimation were obtained from bonding considerations, in which the number of effective bonds that are broken when an atom escapes from a surface are counted. This number and the total number of bonds for each atom within the solid are used to convert the heat of sublimation into surface energy. Williams used a four-layer model, in conjunction with ideal and regular solution models. We show in Figure 6 the calculated concentration profile for a system with a particular bulk concentration and particular relative values of the surface energy difference and regular solution parameter.

TABLE V. Experimental Surface Free Energies of Oxides and Carbides

	σ, ergs/cm^2	T, °K	Method	Comments	Ref
Ag_2O	650			2 mm O_2	22
	600			Ag_2O	22
	$2.28 - 188.1 \log P(O_2) \pm 80$	1205		0.2–0.0001 atm O_2	23
	$2050 - 1.71(T - 273)$			160 mm O_2	24
Al_2O_3	690	2323		Liquid	25
	690 ± 20	2323	Sessile and pendant drop	He atm	26
	680	2323	Shape of drop	5×10^{-5} Torr	27
	680	2323		Liquid	28
	650	2323	Weight of drop	5×10^{-5} Torr	27
	700	2353		Liquid	29
	905 ± 20%	2123		Solid	30
	840			Solid	31
	$892 - 0.12T$			(0001)	32
	925	2143		99.8%	33
B_2O_3	96			Solid	34
	$83 \pm 0.055(T - 1273)$	973–1473			26
	$75.9 + 0.0026(T - 1073)$	1073–1673	Cylinder-drag		35
	$87.4 + 0.004(T - 1213)$	1223–2223	Cylinder-drag		36
BaO	290	1373		Solid	29
	307	2073		Liquid	25
Bi_2O_3	209.7	1097			37
	$232.3 - 0.027(T - 273)$	1103–1173	Maximum bubble pressure		37
CaO	820	298			25
CdO	500	623–1073			38
Cu	1370	1423	Resting drop	0.00 wt % O_2	39
	1270	1423	Resting drop	0.04 wt % O_2	39
	1255	1423	Resting drop	0.08 wt % O_2	39
	825	1423	Resting drop	0.28 wt % O_2	39
	670	1423	Resting drop	0.33 wt % O_2	39
	625	1423	Resting drop	0.63 wt % O_2	39
	530	1423	Resting drop	0.88 wt % O_2	39
FeO	590				34
	585	1693			40
	725	1573–1673			41
	680–700	1573–1673			42
	732			Solid	43
	630 ± 2%	1673	Stationary drop		44
	$7362 - 3.44T$			10^{-3}% O_2	45
	$692 + 0.54T$			0.25% O_2	45
	1050	1683		Liquid	46
	1055	1683		Liquid	43
Fe_3O_4	400	Mp			28
	400		Shape of drop		27
	360		Weight of drop		27
GeO_2	$250 + 0.056(T - 1423) \pm 7\%$	1373–1673	Sessile and pendant drop	He atm	26
In	652	160	Sessile drop	10^{-6} Torr O_2	47
	80–500	160	Sessile drop	1 Torr O_2	47
MgO	1200	77	Cleavage	Limited no. of expts	48
	1000	298	ΔH soln		48
	1150 ± 80	298	Cleavage		48
	1100	1870		99.2% pure	33
MnO_2	620 ± 2%	2123	Stationary drop		44
	653				49
MoO_3	50	Mp	Shape of drop		27
	65	Mp	Weight of drop		27
	70	Mp			28
Na	$186 - 0.1(T - 371)$	371–453	Vertical plate	1–20 $\times 10^{-4}$ Torr O_2	50
	$190.8 - 0.1(T - 371) \pm 1.5\%$	371–723	Max bubble pressure	No oxide	51
	$202 - 0.1(T - 371)$	371–493	Drop volume	No oxide	52
OsO_4	$49.24 - 0.15(T - 361)$	361			53
P_2O_5	$60 - 0.033(T - 373) \pm 7\%$	373–773	Sessile and pendant drop	He atm	26
PbO	132	1173	Anchor ring		54
	134	1273			54
	153	1273	Maximum bubble pressure		55
Re_2O_7	32.2	604	Capillary rise		56
	$35.9 - 0.12(T - 574.5) + 2.3 \times 10^{-5}(T - 574.5)^2$	603–798			57
SiO_2	605	298		Solid	25

TABLE V (Continued)

	σ, ergs/cm^2	T, °K	Method	Comments	Ref
	390 ± 2%	2063	Stationary drop		44
	307 + 0.031(T − 2073)	1273–1573	Sessile drop	He atm	26
Ta_2O_3	280	Mp	Shape of drop		27
	360	Mp	Weight of drop		27
Ta_2O_5	280	Mp			28
TiO_2	355 − 0.174(T − 2125) ± 6%	2125–2600	Cylinder-drag	99.5% pure	58
	280		Shape of drop	5 x 10^{-5} Torr	27
	360		Weight of drop	5 x 10^{-5} Torr	27
	380	Mp			28
UO_2	754 ± 150	1773	Sessile drop	In 99.9995% Ar atm	59
	600 ± 50	973		U/O 2, Ar and O_2 atm	60
	626			Stoichiometric solid	61
	510	1323	Sessile drop		62
V_2O_5	86	1273			55
	90	Mp			28
	90		Shape of drop		27
	95		Weight of drop		27
WO_3	100	Mp			28
WO_2	100		Shape of drop		27
	90		Weight of drop		27
ZnO	90		Rupture	Seems to low	63
ZrO_2	1130	<1423	Phase change	Monoclinic solid	64
	770	1423–2573	Phase change	Tetragonal solid	65
	<770	>2573	Phase change	Cubic solid	65
	800	1870		92.57% pure	33
	590 ± 20%	2123	Sessile drop	He atm	30
HfC	1825 ± 150	1773	Multiphase Equilibrium		66
NbC	2440	1423	Sessile drop	Under 10^{-5} Torr	67
	2300 ± 50	1823	Multiphase Equilibrium		66
TaC	1804 ± 706			Solid	68
	2690	1423	Sessile drop	Under 10^{-5} Torr	67
	1290 ± 390	1373	Sessile drop		69
TiC	1190 ± 350	1373	Sessile drop		69
	2135 ± 150	1723	Multiphase Equilibrium		66
UC	728 − 0.01(T − 1598) ± 41	1598–1993	Sessile drop	Ar atm	70
	1000 ± 300	1373	Sessile drop		69
VC	2200 ± 200	296	Cleavage	C/V = 0.88	71
	3150 ± 300	296	Cleavage	C/V = 0.84	71
	2850 ± 300	296	Cleavage	C/V = 0.76	71
	1677	1423	Sessile drop	Under 10^{-5} Torr	67
	1675 ± 500	1373	Sessile drop		69
	2310 ± 150	1723	Multiphase Equilibrium		66
WC	2820 ± 30	1423	Sessile drop	Under 10^{-5} Torr	67
ZrC	310	1423	Sessile drop	Under 10^{-5} Torr	67
	800 ± 250	1373	Sessile drop		69

The first feature that is observed is that the fourth layer has nearly the same concentration as the bulk, even for this case in which the surface energy difference gives a very large surface effect. The second observation is that the sign of the regular solution parameter is very important in predicting the concentration of the second and third layers. For a positive regular solution parameter, all layers are enriched with the component that has the smallest surface energy. For a negative regular solution parameter, however, there is a depletion in the second layer of the component which is present in excess in the first layer. This effect is very important to the interpretation on Auger results. If the regular solution parameter is zero, then the four layer model reduces to the monolayer model.

In all of these models, it was assumed that there were no impurities present on the surface. The models as discussed above referred to a vacuum interface, or to a surface in equilibrium with its own vapor and neglected the possible existence of a third gaseous phase. In any real "vacuum" interface there is inevitably an ambient, however low the pressure, which is a source of impurities such as CO and H_2O, which may chemisorb on the surface. Under these conditions, the binary solid system becomes actually a ternary system. The bonding characteristics of this third component alters the surface forces and thus completely changes the equilibrium configuration of the surface even though the third component may be of a negligible amount or absent in the bulk. The chemisorbed species may form strong bonds with one of the components and may not bond at all with the other components. In such circumstances, the energy could be lowered by a segregation of the bonding component to the surface. Thus, such a pseudo-binary system would have a surface composition that may be totally different from the same system without the chemisorbed impurity. Such effects can be very large in some cases, and in fact enrichments due to chemisorption have been observed experimentally, as will be seen later.

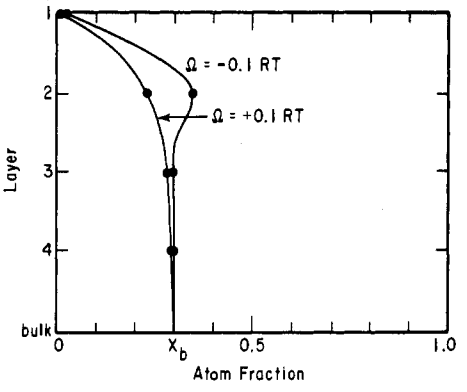

Figure 6. Concentration profile of a fcc (111) face for a regular solution as calculated by Williams (ref 6). In this calculation $\Delta H_{sub} = 10RT$ (which is equivalent to $\Delta\sigma = 3RT/a$) and $\Omega = \pm 0.1RT$.

This then underscores the importance of having a clean surface when making studies of binary systems.

In addition, impurities dissolved in the bulk may also segregate out at the surface. This occurs, if for no other reason, because of the temperature dependence of their solubility in the solid solution. The surface tension may change markedly in the presence of a monolayer of carbon, for example, that induces redistribution of surface atoms which leads to drastic changes in surface composition. Again, in the presence of segregated surface impurities that emanate from the bulk, the binary system is converted to a ternary system. Since carbon and sulfur are the most common impurities in metals that are likely to segregate at surfaces, their effects on the surface composition should be explored.

V. Summary of Experimental Determination of Surface Composition by Auger Electron Spectroscopy

With the advent of Auger electron spectroscopy (AES) it has become possible to determine not only the type of atoms on a surface, but also to carry out semiquantitative determinations of the relative atom concentrations in the first few layers. As a result, several laboratories are now engaged in measuring the surface compositions of various binary alloy systems. In this section we shall first very briefly review the techniques of AES and discuss its capabilities and limitations. Next we will discuss how the technique has been applied to determine surface phase diagrams of binary alloy surfaces and the results of these investigations.

When an energetic beam of electrons or X-rays (1000–5000 eV) strikes the atoms of a material, electrons which have binding energies less than the incident beam energy may be ejected from the inner atomic levels. By this process a singly ionized excited atom is created. The electron vacancy thus formed is filled by deexcitation of electrons from higher electron energy states that fall into the vacancy. The energy released in the resulting electronic transition can, by electrostatic interaction, be transferred to still another electron (in the same atom or in a different atom). If this electron has a binding energy that is less than the deexcitation energy transferred to it, it will then be ejected into vacuum, leaving behind a doubly ionized atom. The electron that is ejected as a result of this deexcitation process is called an Auger electron, and its energy is primarily a function of the energy level separations in the atom.[83,84] The electrons that are emitted are therefore characteristic of the types of atoms from which they are emitted, and energy analysis of these electrons therefore can give qualitative information of the surface of the solid.

Solids have quite large inelastic and elastic electron scattering cross-sections. It is the high scattering cross-section of these fairly low-energy electrons that makes AES a surface-sensitive technique; only electrons emitted within a few monolayers of the surface will escape without energy loss. However, emitted along with the Auger electrons there will be a broad background of secondary electron emission and energy loss peaks. It was this large background that hindered the use of AES as a surface analysis technique for many years. However, in 1968 Harris[85] applied a method of electronic differentiation to the previously recorded $N(E)$ curves. This differentiation served to greatly enhance the sensitivity. As an example, in Figure 7 we have shown examples of typical differentiated and undifferentiated spectra. The peak labels used are the standard X-ray notations,[86] with V representing the valence band. Note that the $M_{23}VV$ peak, which is on a steep background in the $N(E)$ curve, is greatly enhanced in the $dN(E)/dE$ curve. Since the development of this method, the use of AES for determining surface compositions has grown exponentially. Many workers are using AES routinely in combination with other surface-sensitive techniques, and review papers have been written on this subject.[84,87]

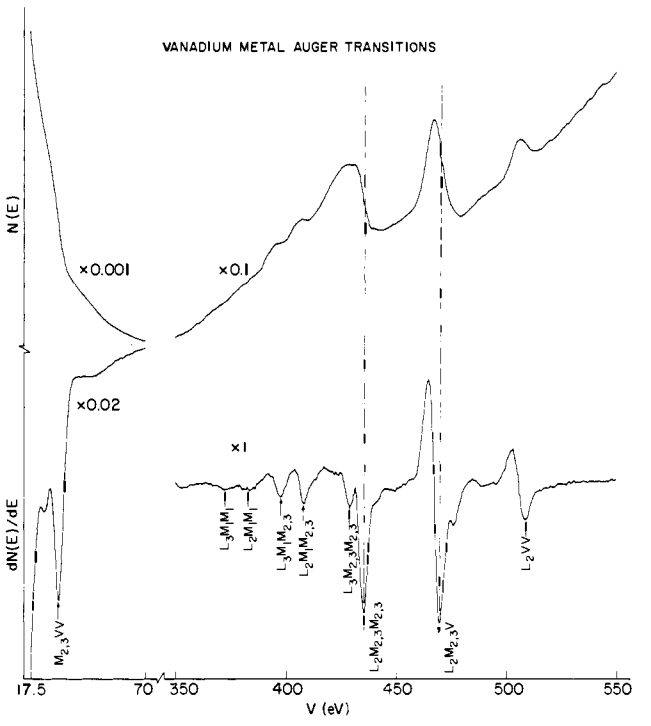

Figure 7. The $N(E)$ and $dN(E)/dE$ Auger spectra of a vanadium metal (100) surface (from Ph.D. Thesis, F. J. Szalkowski, University of California, Berkeley, 1973).

One of the challenges that face workers in the field today is that of making AES into a quantitative technique. The number of Auger electrons emitted at a certain energy is directly proportional to the number of the type of atom emitting at that energy. The intensity I_A of Auger electrons actually collected at a certain energy is given by

$$I_A = (sI_p)T \csc(\phi_p)$$

where I_p is the intensity of the primary electron beam (which is the method commonly used to excite Auger transitions), ϕ_p is the angle of incidence of the primary beam measured from the normal, s is the probability of stimulating an Auger electron and having it escape from the solid, and T, the transmission of the detector, is the probability that an electron emitted from the solid will be collected and "counted".[88]

The factor s, which contains all the information about the system,[89,90] can be written as

$$s = \sigma(E_p)(1 - \omega)\sum_i N_i a_i$$

where $\sigma(E_p)$ is the ionization cross-section which is a function of the energy of the primary electron beam,[91,92] $(1 - \omega)$ is the Auger transition probability,[86] and the summation is over the atomic layers of the solid, the ith layer containing N_i atoms of the emitting type. The terms a_i are attenuation factors for electrons escaping from the ith layer. These factors are dependent upon the depth of the layer, and upon the composition of the surrounding layers due to backscattering and screening effects.

From the above expression, there emerge three basic difficulties in using Auger intensities to obtain a quantitative chemical analysis of the surface of a solid solution. We shall sketch these three problems and list some of the techniques that are being used or that might be used to overcome the difficulties.

The first problem is that of the actual calibration. The first step in the calibration is to remove all obvious instrumental factors from consideration. The spectra should all be run with similar operating conditions. (This includes factors such as the modulating voltage amplitude used in obtaining the differentiated signal, modulation frequency, etc.). The electron current to the crystal can generally be measured and the measured peak-to-peak amplitude (or whatever other quantity is used for the analysis) can be normalized to some particular incident current. Next, since the probability of exciting a particular Auger transition varies in an (as yet) unpredictable manner, some standards must be utilized for comparison. This is generally done by measuring the Auger spectra of the pure components. Peak intensities are measured for each of the Auger transitions that are to be used in the analysis. The intensities are normalized and are then believed to give the surface composition of solid solution by linear interpolation. This linear interpolation assumes that the factors a_i and the Auger transition probabilities are independent of matrix effects.

The second problem that arises is that of which feature of the spectra to use as a measure of the Auger intensity. As stated earlier, the spectra that is generally measured is the $dN(E)/dE$ curve, from which the actual Auger intensity can be obtained only by integration. The quantity that is generally used is the peak-to-peak intensity of the $dN(E)/dE$ curve,[93] or the amplitude of one of the peaks. However, the difficulty is that if the slope of the background changes or if the shape of the Auger peaks changes owing to any concentration or chemical effect, then the peak-to-peak height cannot be expected to be a linear measure of composition.[93-95] The problem has been considered theoretically,[96] and the resulting suggested integration techniques have been applied.[97] If the shape of the $dN(E)/dE$ curve (and therefore the $N(E)$ curve) is shown not to change with composition, the peak-to-peak height is a valid measure of surface composition.[93]

The third problem that is encountered, and perhaps the most difficult to overcome, is the depth distribution problem which arises from the term $\sum_i N_i a_i$ given in the expression for the Auger intensity. The problem arises from the fact that the Auger electrons penetrate one to several monolayers and are attenuated by the complicated a_i factors. So if two Auger transitions of different energies are used for the analysis of the two components, then the sampling depth, or the "detected volume", will be different for the two energies. Thus the Auger peak will be a weighted average over more than one layer. This effect will tend to attenuate surface enrichment effects, such as those discussed earlier. One way this problem can be attacked is to alter the sampling depth in some manner. This may be done by comparing intensities for Auger peaks of various energies from each component. Another way in which the sampling depth may be altered is by varying the angle of incidence of the exciting electrons, or by covering the surface with a layer of noninteracting and nondiffusing atoms. An approach similar to this has been taken to obtain Auger escape depths for samples of Mo on W.[98] Another idea which has been used theoretically, is to compare plasmon satellite intensities with Auger peak intensities as a function of the electron exit angle. This method gives a depth profile of adatom concentration.[99] A great deal more work still needs to be done, however, before it will become possible to measure composition profiles accurately.

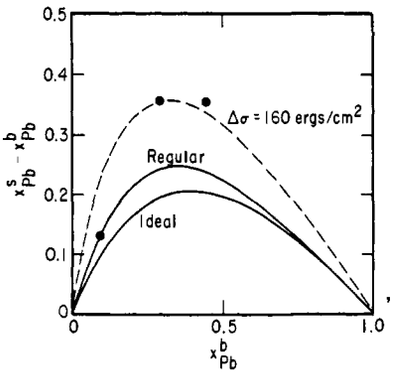

Figure 8. Surface enrichment in Pb–In as predicted by the ideal solution and the regular solution monolayer models at 500°. The dashed line is for an ideal solution with the same surface area as Pb–In at 500°, but with $\Delta\sigma$ = 160 ergs/cm^2. The points are experimental values of Berglund and Somorjai.[100]

Having made the reader aware of the difficulties involved in Auger intensity analysis, we will summarize some of the work that has been carried out to measure the surface composition of alloys.

One system which has been studied is that of the molten Pb–In.[100] This study was done using AES, and a molten system was chosen so that temperature dependence could be studied. The "surface compositions" found are shown in Figure 8 along with values predicted assuming the solution is ideal and values predicted assuming the solution is regular, both in the monolayer approximation. For both molten Pb and molten In the surface tension is known as a function of temperature to be[101]

$$\sigma_{Pb} = 460 - 0.12(T - T_f) \text{ ergs/cm}^2$$

$$\sigma_{In} = 559.2 - 0.089(T - T_f) \text{ ergs/cm}^2$$

where T_f is the melting point of the metal. The regular solution parameter used was Ω = 910 cal/mol as obtained from heat of mixing data.[82] As predicted by the theory, the surface proved to be enriched with lead. However, it was found that the "surface concentration" was even greater in lead than predicted by the monolayer models. It should be borne in mind that the "surface compositions" are obtained from Auger peak intensity, and thus it is subject to all the difficulties involved in relating surface concentrations to Auger intensity data. This extra Pb concentration cannot be attributed to sampling depth problems, because sampling greater than one monolayer would serve to lower the measured concentration of Pb (except in the unlikely event that the first few underlying layers have a very large enrichment in Pb). The temperature dependence of the intensity ratios was determined, and it was found that $\ln(I_{Pb}/I_{In})$ varied linearly with $1/T$, where I is the Auger peak intensity. The ratio I_{Pb}/I_{In} should be proportional to the ratio x_{Pb}^s/x_{In}^s. This then is the result predicted by the monolayer ideal solution model. Thus, this system acts as if it were ideal but with a surface energy difference greater than that obtained from surface tension data (Figure 8). The Ni–Au

binary system has been studied,[6] and an enrichment of the surface with Au was found. The limited data was found to follow, within experimental error, the predicted values calculated by the four-layer model. In addition, it was found that chemisorption had an effect in altering the surface composition. Oxygen and hydrogen both were found to enrich the surface with Ni as predicted from the greater stability of Ni–O and Ni–H bonds than that of Au–O and Au–H bonds.

In a study of Cu–Al,[102] an enrichment of the surface with Al was found, as expected from the heats of sublimation and from surface tension data. In this work Ar sputtering was used as a means of calibrating and cleaning the sample. The surface was bombarded until it was assumed that the resulting unequilibrated surface must have the same composition as the known bulk composition. This assumption may be made only with great care, however, in view of the evidence for highly selective sputtering in many systems.[103,104] In this particular case, Al and Cu have very similar heats of sublimation, so their sputtering may be nearly equal at the energies used. This must, however, be checked carefully.

A system that has been studied exhaustively is the Cu–Ni system. Interesting because of its catalytic properties, the system was studied by work function measurements by Sachtler and Dorgello in 1965.[105] These workers found that there is phase separation at the temperatures they used, and that the Cu-rich phase enveloped the Ni-rich phase, a condition which developed because of the relative diffusion rates of the two components and due to the lower surface tension of copper. After the development of AES, the system was studied by Harris[85] and later by Quinto and workers.[106] They found there to be no indication that the surface composition was different from the bulk composition. The Auger transitions used in this analysis were rather high energy, 715 eV for Ni and 920 eV for Cu and two intermediate energies which were overlapping and unresolved Cu and Ni peaks. Electrons of these energies may be expected to sample more than one monolayer.

These seemingly conflicting results can be reasonably explained by considering the alloy preparation procedure used by the two groups. The films prepared by Sachtler were sintered at low temperatures, whereas Quinto used high-temperature anneals for their bulk alloys, followed by rapid quenching. Thus phase transformation at some intermediate temperature would explain the results of both experiments. This situation calls attention to the importance of knowing the phase diagram for the bulk sample, when trying to understand the surface phase diagrams. In addition to the equilibrated surface of Cu/Ni, the sputtered surface has also been studied using AES[103,107] and the catalytic activity has been studied for the system characterized in this way.[108]

The fact that the Auger intensity ratios for the Cu–Ni system were the same as predicted from the bulk compositions does not necessarily indicate that there was no excess of either component at the surface. Because of the rather large penetration depths expected for electrons of the energies used in the analysis, surface effects may have been attenuated. However, the fact that the Cu to Ni intensity ratios did not change with the angle of incidence of the exciting electron beam, as found by Ertl and Küppers,[109] does seem to be evidence against surface segregation. A grazing incidence beam will sample less deeply than a normal incidence beam. Thus, if there is a concentration profile over the sampled depth, then the Auger intensity ratios will vary with angle of incidence. A similar study was made of the Ag–Pd system, and here also no surface segregation effects were observed for the clean and homogeneous crystalline films.[110]

A study of the Ag–Au system[111] found no evidence of segregation of Ag to the surface as expected from its lower heat of sublimation. In this work, the Auger spectrum was recorded from an epitaxial alloy film grown on a mica substrate. The peak-to-peak height for three different gold peaks of widely varying energies (72, 239, and 2024 eV) were measured and this value divided by the peak-to-peak height of the corresponding Auger signal from pure gold. The approximate escape depths for these energies were estimated to be 4, 8, and 30 Å, respectively. The resulting ratios were found to be approximately equal, indicating no composition gradient over the depths sampled. A silver overlayer (approximately two monolayers) was then evaporated onto the alloy, and it was found to diffuse into the bulk upon annealing at 300° to the extent that within an hour the gold Auger peaks returned to nearly their former intensity.

The system Pt–Sn has also been studied using AES.[112] A study was made of the intermetallic compounds Pt_3Sn and PtSn. The Auger transitions used in the analysis were the Pt peaks at 169 and 236 eV and a Sn peak at 428 eV. An enrichment of Sn was found on the surface for both compounds, a result expected from the lower heat of sublimation of Sn (and therefore lower surface free energy). In addition, they found that chemisorption of O_2 tended to increase the surface concentration of Sn as expected because of the higher stability of tin oxide. Similarly H_2 was found to bring Pt to the surface. The transitions used in this study are expected to be more surface sensitive than those used in the Cu–Ni studies, especially with the glancing incidence gun that was used. Sampling depth was estimated at one to three monolayers, but no attempt was made to sort out the concentration profile. Later, however, the work was extended by adding higher energy transitions in an X-ray photoemission experiment, to get at the composition profile. It was found that there was an enrichment of Sn on the top monolayer and that there was a corresponding depletion of Sn in the underlying layer.[113]

From studies of just a few systems, it is already clear that AES is a powerful technique to study the surface phase diagram of multicomponent systems. It appears that the surface thermodynamics of these important systems can now be explored. As a result, it is likely that new surface phases will be found that exist when there is no corresponding phase existing in the bulk phase diagram and that the surface composition will be markedly different from the bulk composition for most systems. The determination of surface phase diagrams will be an important new research area of surface science.

VI. Addendum

In recent months there has been a very large increase in the number of studies of the composition of alloy surfaces. The results of some of these studies are sketched briefly below.

At least four separate investigations have been carried out on the Cu–Au system. In a study undertaken by Fain and McDavid,[114] Au and Cu were evaporated onto mica substrates yielding homogeneous oriented films. The Auger intensities of three Au peaks of different sampling depth were used to obtain the Au bulk atom fraction and the atom fractions in the first and second layers. Calibration was performed using films of pure Au. The results indicated that the first layer was enriched in Au (for example, $x_{Au}^{b} = 0.5$ gave $x_{Au}^{s} = 0.95$), while the second layer had essentially the same composition as the bulk. The enrichment in Au is opposite that predicted from the heats of sublimation but is in qualitative agreement with the trend predicted from the strain theory.[115] In another study,[116] rods of $AuCu_3$ and Au_3Cu were broken in UHV and the Auger intensity ratios Cu(60 eV)/Au(70 eV) and Cu(920 eV)/Au(2024 eV) were measured. Comparison of the ratios for the two alloys indicated that the ratios reflected the

bulk composition. The ratios for Au_3Cu were found not to vary with temperature up to 600°C. For $AuCu_3$ the ratios were found to increase between 300 and 400°C, but decreased again above 500°C. Segregation of sulfur to the surface was found to occur in the same temperature range, indicating that the presence of S impurities increased the Cu concentration in the surface region. These results seem to indicate that there is no surface segregation for clean equilibrated Au–Cu alloys, which can be rationalized as a cancellation of effects due to surface energy and strain energy. These results were confirmed by Auger in another study.[117] In this work, the surface ordering properties of Cu_3Au were also investigated. However, a fourth Auger spectroscopy study[118] indicated the possibility of enrichment of Au in the surface region, in agreement with Fain and McDavid. Further theoretical attempts at understanding the surface composition of ordered alloys such as observed in Au–Cu alloys have also been made.[119]

More work has been completed on the Cu–Ni system. It has been speculated[120] that a source of confusion has been the use of high-energy Auger peaks in some studies and of the more surface-sensitive low-energy peaks in others. A recent study using low-energy peaks indicated that Cu does segregate at the surface as predicted from its lower heat of sublimation.[121] In another study an attempt has been made at describing the theory of surface segregation at surfaces of small alloy particles.[122] In addition, the same authors present catalytic evidence which gives support to their theory as applied to Cu–Ni.[123]

Studies of various other miscible systems have been completed. A study of Ni–Pd films[124] indicated that there was surface enrichment of Pd, the component with the lower heat of sublimation. These results showed that the use of low-energy Auger peaks was necessary to see the effects of the enrichment. In an Auger study of Au–Ag,[125] it was found by comparison of low-energy and high-energy peaks that there is enrichment of the surface with Ag although the extent of the segregation is less than predicted by the regular solution theory. An Auger study of Fe–Cr[126] indicated surface enrichment of Cr in an alloy of $Fe_{0.84}Cr_{0.16}$. At least two studies of systems with miscibility gaps were made. An Auger spectroscopy analysis of the surfaces of quenched polycrystalline Ag–Cu alloys was made to study the effects of sputtering, cleaving, and scribing on surface composition.[127] Finally, a study of Sachtler and coworkers[128] using a technique of chemisorptive titration supported their "cherry" model and demonstrated that owing to phase separation, the surface composition of Pt–Au alloys was constant throughout the miscibility gap. This is in agreement with earlier work function studies,[129] which seemed to indicate that the Au-rich phase covers the surface throughout a wide range of bulk composition.

Acknowledgment. This work was done under the auspices of the U.S. Atomic Energy Commission through the Inorganic Materials Research Division of Lawrence Berkeley Laboratory.

VII. References

(1) R. Defay, I. Prigogine, A. Bellemans, and D. H. Everett, "Surface Tension and Adsorption," Wiley, New York, N.Y., 1966.
(2) T. P. Hoar and D. A. Melford, *Trans. Faraday Soc.*, **53**, 315 (1957).
(3) J. E. Lane, *Aust. J. Chem.*, **21**, 827–51 (1968).
(4) D. H. Everett, *Trans. Faraday Soc.*, **61**, 2478 (1965).
(5) A. R. Alterbenger and J. Steckl, *Chem. Phys. Lett.*, **5**, 29 (1970).
(6) F. L. Williams, Ph.D. Thesis, Stanford University, 1972.
(7) R. A. Swalin, "Thermodynamics of Solids," 2nd ed, Wiley, New York, N.Y., 1972.
(8) J. H. Hildebrand, J. M. Prausnitz, and R. L. Scott, "Regular and Related Solutions," Van Nostrand Reinhold, New York, N.Y., 1970.
(9) E. D. Hondros in "Techniques of Metals Research," Vol. IV, Part 2, R. A. Rapp, Ed., Interscience Publishers, N.Y., 1970.
(10) R. V. Eötvös, *Wied Ann.*, **27**, 456 (1886).
(11) W. Ramsey and J. Shields, *J. Chem. Soc.*, 1089 (1893).
(12) M. Katayama, *Sci. Rep. Tohoku Imp. Univ.*, **4**, 373 (1916).
(13) J. S. Vermaak and D. Kuhlmann-Wilsdorf, *J. Phys. Chem.*, **72**, 4150 (1968).
(14) E. A. Guggenheim, *J. Chem. Phys.*, **13**, 253 (1945).
(15) H. Jones, *Met. Sci. J.*, **5**, 15 (1971); A. V. Grosse, *J. Inorg. Nucl. Chem.*, **26**, 1349 (1964).
(16) B. C. Allen, *Trans. Met. Soc. AIME*, **227**, 1175 (1963).
(17) J. Bohdansky and H. E. J. Schins, *J. Inorg. Nucl. Chem.*, **29**, 2173 (1967).
(18) A. S. Skapski, *J. Chem. Phys.*, **16**, 389 (1948).
(19) D. McLachan, *Acta Metall.*, **5**, 111 (1957).
(20) J. J. Bikermann, *Phys. Status Solidi*, **10**, 1 (1965).
(21) G. J. Janz, G. R. Lakshminarayanan, R. P. T. Tompkins, and J. Wong, "Molten Salts," Vol. 2, Sec. 2, *Nat. Stand. Ref. Data Ser., Nat. Bur. Stand.*, NBS-28 (1969).
(22) *Poverkhn. Yavleniya Met. Splavakh Ikh Rol Protsessakh Poroshk. Metall., Akad. Nauk Ukr. SSR*, 100 (1961).
(23) F. H. Buttner, E. R. Funk, and H. Udin, *J. Phys. Chem.*, **56**, 657 (1952).
(24) J. A. Allen, *Aust. J. Chem.*, **13**, 210 (1960).
(25) R. Panpuch, *Sillc. Ind.*, **23**, 191 (1958).
(26) W. D. Kingery, *J. Am. Ceram. Soc.*, **42**, 6 (1959).
(27) *Poverkh. Yavleniya Rasplavakh*, 155 (1968).
(28) V. I. Kostikov, M. A. Maurakh, B. S. Mitin, I. A. Pen'kov, and G. M. Sverdlov, *Sb., Mosk. Inst. Stali Splavov*, No. 49, 106 (1968).
(29) W. D. Kingery, *Metallurg (Moscow)* 446 (1963).
(30) W. D. Kingery, *J. Am. Ceram. Soc.*, 37, 42 (1954).
(31) A. Portevin and P. Bastien, *C. R. Acad. Sci.*, **202**, 1072 (1937).
(32) S. K. Rhee, *J. Am. Ceram. Soc.*, **55**, (6), 300 (1972).
(33) P. P. Budnikov and F. Y. Xaritonov, *Izv. Akad. Nauk SSSR, Neorg. Mat.*, **3** (3), 496 (1967).
(34) S. I. Popel and O. A. Eisen, *Zh. Neorg. Khim.*, **2**, 632 (1957).
(35) L. Shartsis and R. Canga, *J. Res. Nat. Bur. Stand.*, **43**, 221 (1949).
(36) E. E. Shpil'rain, K. A. Yakimovich, and A. F. Tsitsarkin, *High Temp.-High Pressures*, **4**, 67(1972).
(37) I. D. Sokolova and N. K. Voskrecenskaya, *Izv. Akad. Nauk SSSR, Neorg. Mat.*, **6** (7), 1358 (1970).
(38) R. Fricke and F. Blaschke, *Z. Electrochem.*, **46**, 46 (1940).
(39) V. N. Eremenko, Yu. V. Naidikh, and A. A. Nosonovitch, *Zh. Fiz. Khim.*, **34**, 1018 (1960).
(40) P. Kozakevitch, *J. Chim. Phys.*, **47**, 24 (1950).
(41) C. E. Popel and O. A. Esin, *Zh. Fiz. Khim.*, **30**, 1193 (1956).
(42) T. Wu, A. F. Vishkarev, and V. I. Yavoiskii, *Izv. Vyssh. Uchebn. Zaved., Chern. Metall.*, **6** (1), 27 (1963).
(43) M. D. Chadwick, *Scr. Metall.*, **3**, 871 (1969).
(44) S. I. Popel, V. I. Sokolov, and O. A. Esin, *Zh. Fiz. Khim.*, **43** (12), 3175 (1969).
(45) B. Sikora, *Pr. Inst. Hutn.*, **20** (6), 375 (1968).
(46) E. D. Hondros, *Acta Metall.*, **16**, 1377 (1968).
(47) R. G. Aldrich and D. V. Keller, Jr., *J. Phys. Chem.*, **72**, (4), 1092 (1968).
(48) A. R. C. Westwood and D. I. Goldheim, *J. Appl. Phys.*, **34** (11), 3335 (1963).
(49) R. Boni and G. Derge, *J. Met.*, **8**, 53 (1956).
(50) C. C. Addison, D. H. Kerridge, and J. Lewis, *J. Chem. Soc.*, 2861 (1954).
(51) J. W. Taylor, *J. Inst. Met.*, **83**, 143 (1954).
(52) C. C. Addison, W. E. Addison, D. H. Kerridge, and J. Lewis, *J. Chem. Soc.*, 2262 (1955).
(53) E. Ogawa, *Bull. Chem. Soc. Jpn.*, **6**, 302 (1931).
(54) L. Shartsis, S. Spinner, and A. W. Smock, *J. Am. Ceram. Soc.*, **31**, 23 (1948).
(55) B. M. Lepinskikh, O. A. Esin, and G. A. Teterin, *Zh. Neorg. Khim.*, **5** (3), 642 (1960).
(56) H. V. A. Briscoe, P. L. Robinson, and A. J. Rudge, *J. Chem. Soc.*, 2673 (1932).
(57) L. A. Nisel'son, R. K. Nikolaev, I. I. Vasilevskaya, and A. G. Vasileva, *Zh. Neorg. Khim.*, 1136 (1969).
(58) B. S. Mitin and Yu. A. Nagibin, *Izv. Akad. Nauk SSSR, Neorg. Mat.*, **7** (5), 814 (1971).
(59) R. J. Bratton and C. W. Beck, *J. Am. Ceram. Soc.*, **58** (8), 379 (1971).
(60) J. G. Eberhart, *J. Nucl. Mater.*, **25**, 103 (1968).
(61) P. S. Maiya, *J. Nucl. Mater.*, **40** (1), 57 (1971).
(62) P. Murray, *Plansee Proc., Pap. Plansee Semin., "De Re Met.", 2nd, 1955*, 375 (1956).
(63) P. C. Bonsall, D. Dollimore, and J. Dollimore, *Proc. Brit. Ceram. Soc.*, No. 6, 61 (1966).
(64) R. C. Garvie, *J. Phys. Chem.*, **69**, 1238 (1965).
(65) Yu. M. Polezhaev, *Zh. Fiz. Khim.*, **41**, 2958 (1967).
(66) R. Warren and M. B. Waldron, *Nature (London), Phys. Sci.*, **235** (56), 73 (1972).
(67) D. A. Mortimer and M. Nicholas, AERE-M 2247.
(68) S. K. Rhee, *J. Am. Ceram. Soc.*, **55** (3), 157 (1972).
(69) P. Murray, *Powder Metall.*, **5**, 64 (1960).
(70) E. N. Hodkin, D. A. Mortimer, M. G. Nicholas, and D. M. Poole, *J. Nucl. Mater.*, **39**, 59 (1971).
(71) R. K. Govila, *Acta Metall.*, **20** (3), 447 (1972).
(72) J. E. Brophy, R. M. Rose, and J. Wulff, "The Structure and Properties of Materials," Vol. II, "Thermodynamics of Structure," Wiley, New York, N.Y., 1964, p 51.
(73) R. A. Orlani, *J. Chem. Phys.*, **18**, 575 (1950).
(74) A. Brager and A. Schukowitsky, *Acta Physicochim. URSS*, **21**, 1001 (1946).
(75) H. B. Huntington, *Phys. Rev.*, 81, 1035 (1951).
(76) K. Huang and G. Wyllie, *Proc. Phys. Soc., London, Sect. A*, **62**, 180 (1949).

(77) P. Hohenberg and W. Kohn, *Phys. Rev. B*, **136**, 864 (1964).
(78) W. Kohn and L. J. Sham, *Phys. Rev. A*, **137**, 1697 (1965).
(79) N. D. Lang and W. Kohn, *Phys. Rev. B*, **1**, 4555 (1970).
(80) J. Schmit and A. A. Lucas, *Solid State Commun.*, **11**, 415 (1972).
(81) J. Schmit and A. A. Lucas, *Solid State Commun.*, **11**, 419 (1972).
(82) R. Hultgren, R. L. Orr, P. D. Anderson, and K. K. Kelly, "Selected Values of Thermodynamic Properties of Metals and Alloys," Wiley, New York, N.Y., 1963.
(83) E. H. Burhop, "The Auger Effect and Other Radiationless Transitions," The University Press, Cambridge, 1952.
(84) G. A. Somorjai and F. J. Szalkowski, "Advances in High Temperature Chemistry," Vol. 4, L. Eyring, Ed., Academic Press, New York, N.Y., 1971.
(85) L. A. Harris, *J. Appl. Phys.*, **39**, 1419 (1968).
(86) W. Bambynek et al., *Rev. Mod. Phys.*, **44**, 716–813 (1972).
(87) C. C. Chang, *Surf. Sci.*, **25**, 53–79 (1971).
(88) F. Meyer and J. J. Vrakking, *Surf. Sci.*, **33**, 271–294 (1972).
(89) T. E. Gallon, *J. Phys. D*, **5**, 822–832 (1972).
(90) J. J. Vrakking and F. Meyer, *Surf. Sci.*, **35**, 34 (1973).
(91) D. Smith and T. E. Gallon, *J. Phys. D*, **7**, 151 (1974).
(92) M. Gryzinski, *Phys. Rev. A*, **138** (2A), 336 (1965).
(93) R. E. Weber and A. L. Johnson, *J. Appl. Phys.*, **40**, 314 (1969).
(94) T. W. Haas and J. T. Grant, *Appl. Phys. Lett.*, **16**, 172 (1970).
(95) N. J. Taylor, *Rev. Sci. Instrum.*, **40** (6), 792 (1969).
(96) J. E. Houston, *Surf. Sci.*, **38**, 283 (1973).
(97) J. T. Grant, T. W. Hass, and J. E. Houston, *Phys. Lett. A*, **45**, 309 (1973).
(98) M. L. Tarng and G. K. Wehner, *J. Appl. Phys.*, **44**, 1534 (1973).
(99) P. J. Feibelman, *Phys. Rev. B*, **7** (6), 2305 (1973).
(100) S. Berglund and G. A. Somorjai, *J. Chem. Phys.*, **59**, 5537 (1973).
(101) U. B. Lazarev, *Teor. Eksp. Khim.*, **3**, 504 (1967).
(102) J. Ferrante, *Acta Metall.*, **19**, 743 (1971).
(103) M. L. Tarng and G. K. Wehner, *J. Appl. Phys.*, **42**, 2449 (1971).
(104) M. L. Tarng and G. K. Wehner, *J. Appl. Phys.*, **43**, 2268 (1972).
(105) W. M. H. Sachtler and G. I. H. Dorgello, *J. Catal.*, **4**, 654–664 (1965).
(106) D. T. Quinto, V. S. Sundaram, and W. D. Robertson, *Surf. Sci.*, **28**, 504 (1971).
(107) S. M. Ono, and K. Nakayama, *Surf. Sci.*, **36**, 817 (1973).
(108) M. Ono, Y. Takasu, K. Nakayama, and T. Yamashina, *Surf. Sci.*, **26** 313 (1971).
(109) G. Ertl and J. Küppers, *J. Vac. Sci. Technol.*, **9**, 829 (1971).
(110) K. Christmann and G. Ertl, *Surf. Sci.*, **33**, 254 (1972).
(111) S. C. Fain, Jr., and J. M. McDavid, *Phys. Rev. B*, **9**, 5099 (1974).
(112) R. Bouwman, L. H. Toneman, and A. A. Holscher, *Surf. Sci.*, **35**, 8 (1973).
(113) R. Bouwman and P. Biloen, *Surf. Sci.*, **41**, 348 (1974).
(114) J. M. McDavid and S. C. Fain, Jr., *Surf. Sci.*, submitted for publication.
(115) D. McLean, "Grain Boundaries in Metals," Clarendon Press, Oxford, 1957.
(116) R. A. Van Santen, L. H. Toneman, and R. Bouwman, *Surf. Sci.*, **47**, 64 (1975).
(117) V. S. Sundarem, R. S. Alben, and W. D. Robertson, *Surf. Sci.*, **46**, 653 (1974).
(118) J. M. Blakely and H. C. Potter, *J. Vac. Sci. Technol.*, to be published.
(119) R. A. Van Santen and W. M. H. Sachtler, *J. Catal.*, **33**, 202 (1974).
(120) F. L. William and D. Nason, *Surf. Sci.*, **45**, 377 (1974).
(121) C. R. Helms, *J. Catal.*, **36**, 114 (1975).
(122) J. J. Burton, E. Hyman, and D. G. Fedak, *J. Catal.*, to be published.
(123) J. J. Burton and E. Hyman, *J. Catal.*, to be published.
(124) C. T. H. Stodart, R. L. Moss, and D. Pope, *Surf. Sci.*, to be published.
(125) S. H. Overbury and G. A. Somorjai, to be published.
(126) C. Leygraf, G. Hultquist, and S. Ekelund, *Surf. Sci.*, **46**, 157 (1974).
(127) P. Braun and W. Färber, *Surf. Sci.*, **47**, 57 (1975).
(128) F. J. Kuijers, R. P. Dessing, and W. M. H. Sachtler, *J. Catal.*, **33**, 316 (1974).
(129) R. Bouwman and W. M. H. Sachtler, *J. Catal.*, **19**, 127 (1970).